Electronic Supplementary Material (ESI) for Journal of Materials Chemistry A.
This journal is © The Royal Society of Chemistry 2015

Supporting Information

Heterogeneous Rhodium-Tin Nanoparticles: Highly Active and Durable Electrocatalysts for the Oxidation of Ethanol

Minjeh Ahn,[a] In Young Cha,[b] Joong Kee Lee,[a] Sung Jong Yoo*[b] and Yung-Eun Sung*[cd]

[a] Green City Technology Institute, Korea Institute of Science and Technology, Seoul, 136-791, Korea.

[b] Fuel Cell Research Center, Korea Institute of Science and Technology, Seoul, 136-791, Korea.

[c] School of Chemical and Biological Engineering, Seoul National University, Seoul, 151-742, Korea.

[d] Center for Nanoparticle Research, Institute for Basic Science, Seoul, 151-742, Korea.

Corresponding authors

ysung@snu.ac.kr (Y.-E. Sung)

ysj@kist.re.kr (S. J. Yoo)

Contents

Experimental works

Synthesis of carbon supported heterogeneous Rh–Sn nanoparticles: Carbon black powders were dispersed in ethylene glycol under agitation for 30 minutes, after which the mixtures were stirred for 1 hour. Ethylene glycol, containing the appropriate quantities of Rh(III) chloride and Sn(II) chloride for various ratios, were poured into the previously prepared solutions. The suspensions were submitted to microwave radiation with 140 W for 10 minutes at 170 °C to reduce the metal precursors. This was followed by filtration by ethanol, and drying in an oven at 75 °C overnight. The carbon-supported Rh–Sn nanoparticles were heated at 160 °C under a reducing atmosphere for 1 hour to remove any unreacted metallic precursors. All of the samples contained 20 wt % of metal; the molar ratios Rh/Sn varied. Commercial 20 wt % Pt/C (Johnson Matthey Co.) catalyst was served as a reference.

Electrochemical and Physical characterizations: Electrochemical activities were evaluated in a standard three-electrode electrochemical cell using an AUTOLAB potentiostat. A platinum wire and Ag/AgCl electrode were utilized as a counter electrode and reference electrode, respectively. All electrochemical data were recorded versus a reversible hydrogen electrode (RHE) after calibration of the pH dependence. 5 μl of catalyst slurry was dropped onto the glassy carbon electrode as a working electrode, and loading amounts of sample were approximately 0.25 mg cm^{-2}. Cyclic voltammograms were recorded at room temperature in an oxygen-free 0.1 M potassium hydroxide, containing various concentrations of ethanol, at a scan rate of 20 mV s^{-1}. To measure the durability of the catalysts with regard to the oxidation of ethanol, the chronoamperometric measurements were also conducted in the identical electrolyte at a constant potential of 0.3 V for 1 hour. Electrochemical surface areas were estimated using carbon monoxide displacement in 0.1 M potassium hydroxide electrolyte. When electrochemical data for the Tafel plots were acquired, the scan rate was set to 1 mV s^{-1} to more precisely obtain values for the oxidation of ethanol. Accelerated stability test was measured through the electrochemical potential cycling for 1000 cycles in an oxygen-free 0.1 M potassium hydroxide from 0.6 V to 1.0 V, at a scan rate of 50 mV s^{-1}.

High-resolution transmission electron microscopy (HR-TEM) was performed using a JEM-2100F at an accelerating voltage of 200 kV. Cs-corrected scanning transmission electron microscopy (STEM) was conducted using a JEM-ARM200F (200 kV, JEOL) equipped with an energy-dispersive X-ray spectroscope (EDS; Bruker Quantax 400).

High-resolution X-ray photoelectron spectroscopy (HR-XPS) measurements were performed on the soft-X-ray beam line, which was connected to an undulator (U7) at the 8A1 beam line of the Pohang Accelerator Laboratory. The experiments were carried out in an ultrahigh vacuum (UHV) chamber with a base pressure $\leq 5 \times 10^{-10}$ Torr using incident photon energies of 630 eV and 1000 eV. Curve fitting was done with the AVANTAGE program.

X-ray absorption near-edge structure (XANES) experiments were performed at the 7D beam line of the Pohang Accelerator Laboratory (3.0 GeV of storage-ring energy, 230 mA with top-up mode) using photon energies ranging from 4 to 30 keV using a bending magnet as the source. The incident beam was monochromated using a Si(111) double-crystal monochromator. The Rh K-edge (E_0 = 23,220 eV) spectra were obtained in transmission mode with separate He-filled IC Spec ionization chambers for incident and transmitted beams. The acquired results were analyzed with ATHENA and ARTEMIS in the suite of IFEFFIT software programs.

The *in situ* ATR-FTIR measurements (Thermo Scientific) were acquired with a spectrometer with a mercury cadmium telluride (MCT, HgCdTe) detector and a germanium crystal prism, using unpolarized infrared radiation. The spectral resolution, angle of incidence, and number of scans were set to 4 cm^{-1}, 60 °, and 6, respectively, and the spectra were collected in series collection mode to observe the spectra with applied potentials in real time. The band intensities were normalized to the ratios of maximum (the point at the most CO_2 produced for the Rh_3Sn_7/C catalyst) and minimum (CO_2-free conditions under steady-state). The results were attained at constant temperature (room temperature) in an oxygen-free 0.5 M ethanol electrolytes at a scan rate of 20 mV s^{-1}.

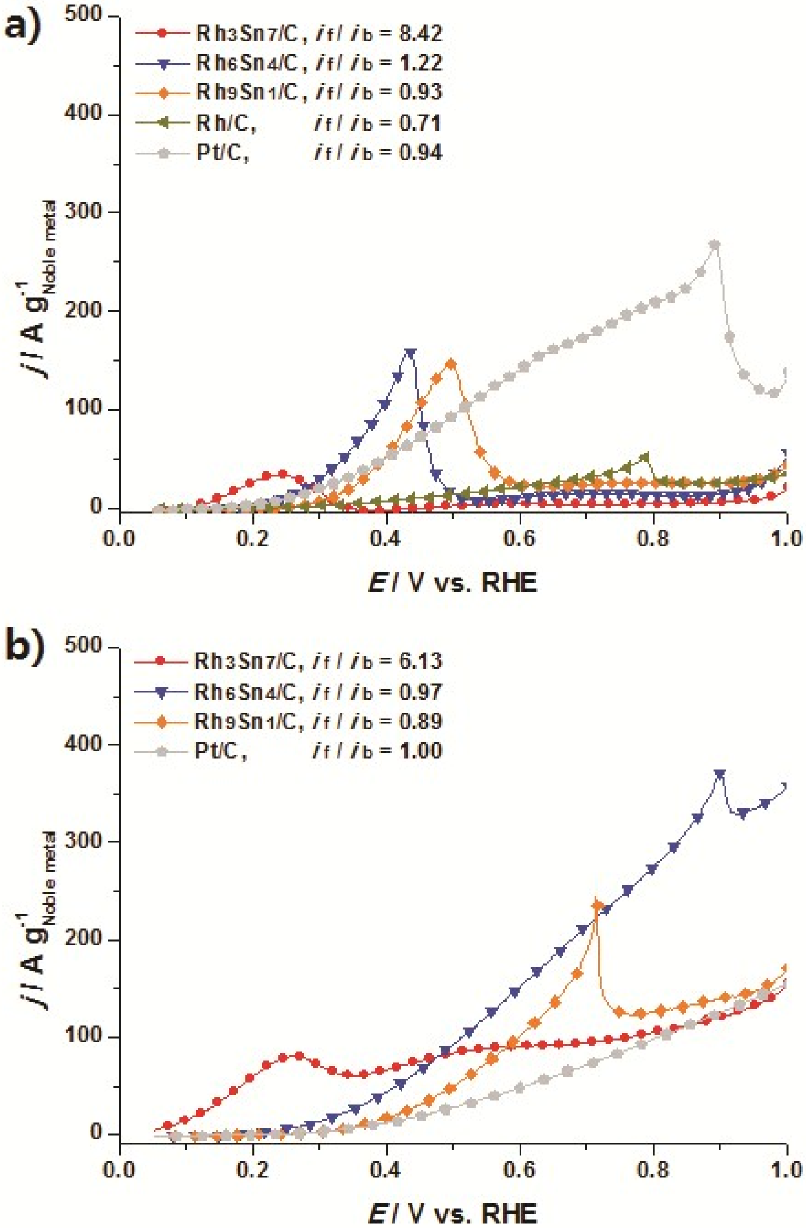

Figure S1. Voltammetric profiles (backward scan) of Rh-Sn catalysts and commercial Pt catalyst for the electrooxidation of ethanol in an Ar-purged 0.1 M potassium hydroxide containing a) 0.5 M ethanol and b) 6.0 M ethanol at a scan rate of 20 mV s^{-1}.

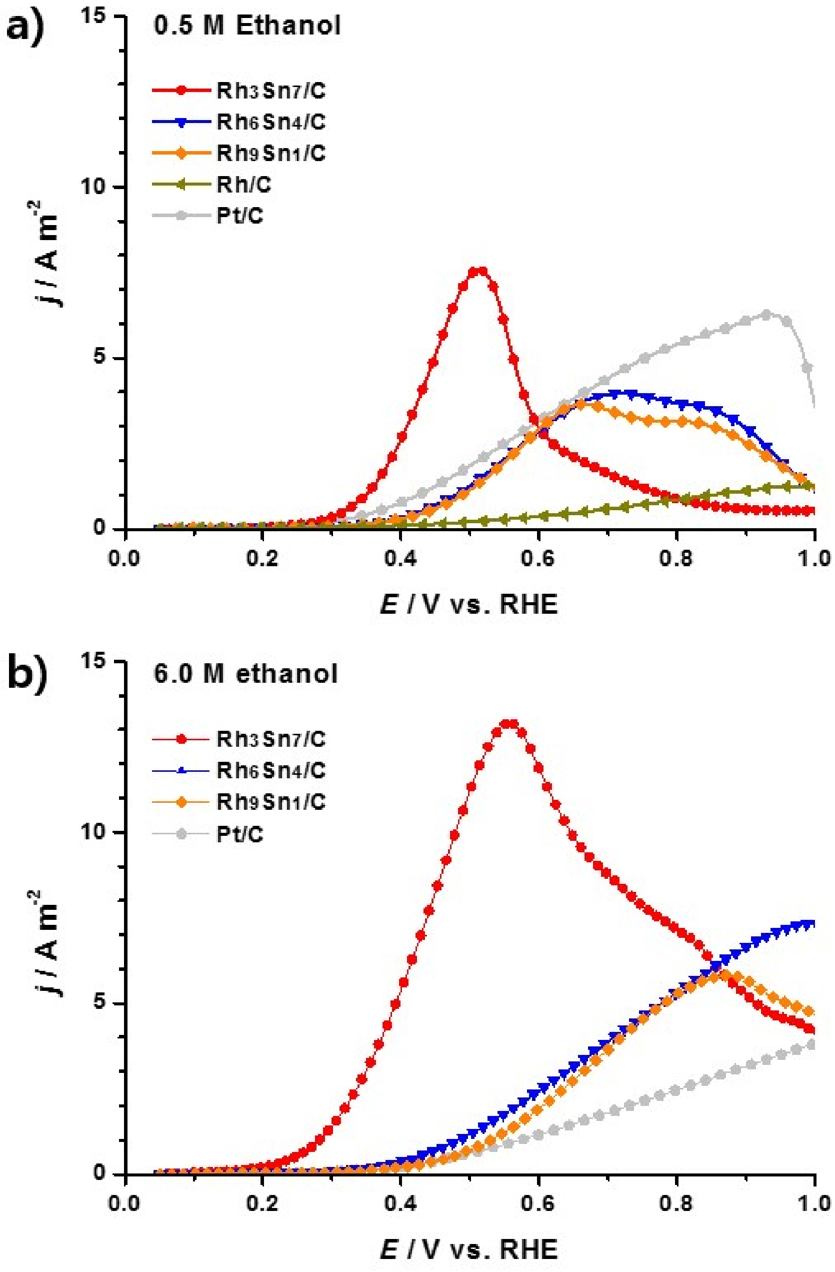

Figure S2. Area-specific current densities of Rh-Sn catalysts and commercial Pt catalyst for the electrooxidation of ethanol in an Ar-purged 0.1 M potassium hydroxide containing a) 0.5 M ethanol and b) 6.0 M ethanol at a scan rate of 20 mV s^{-1}.

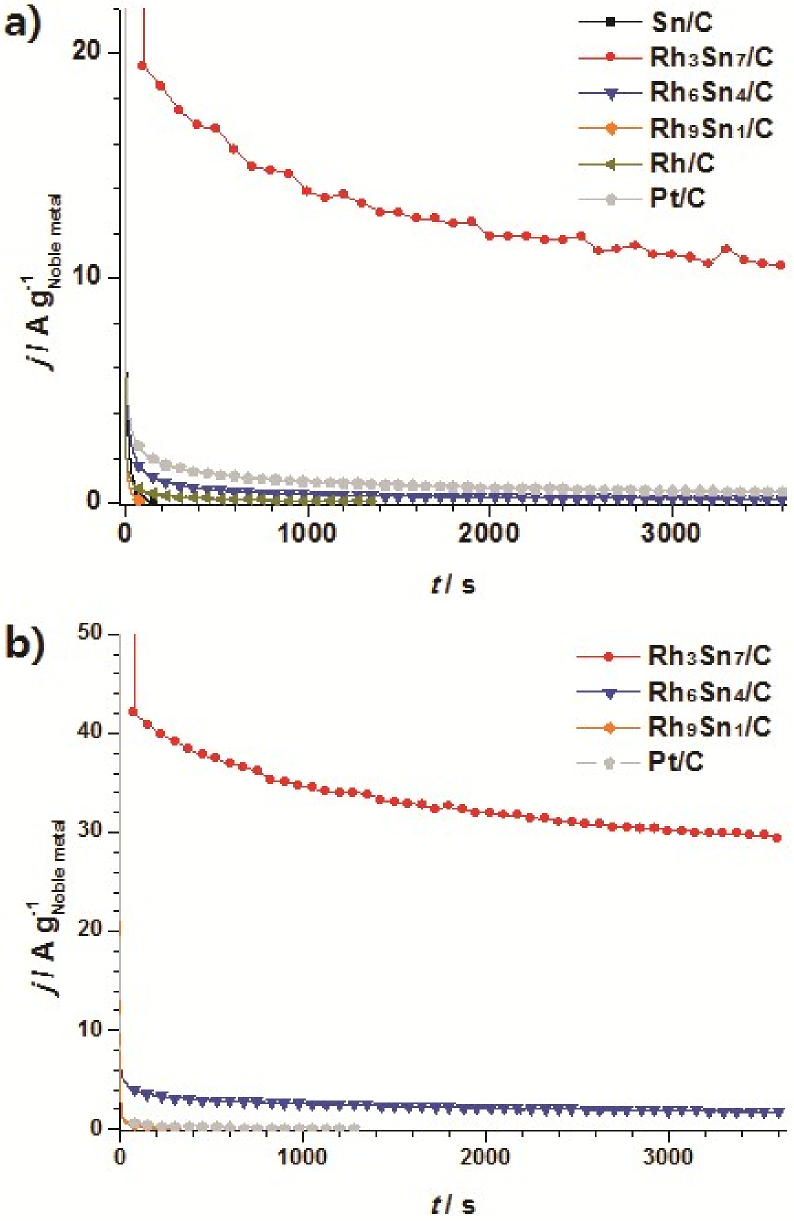

Figure S3. Chronoamperometry results of Rh-Sn catalysts and commercial Pt catalyst at a constant potential of 0.3 V for 1 hour in a) 0.5 M ethanol and b) 6.0 M ethanol electrolyte.

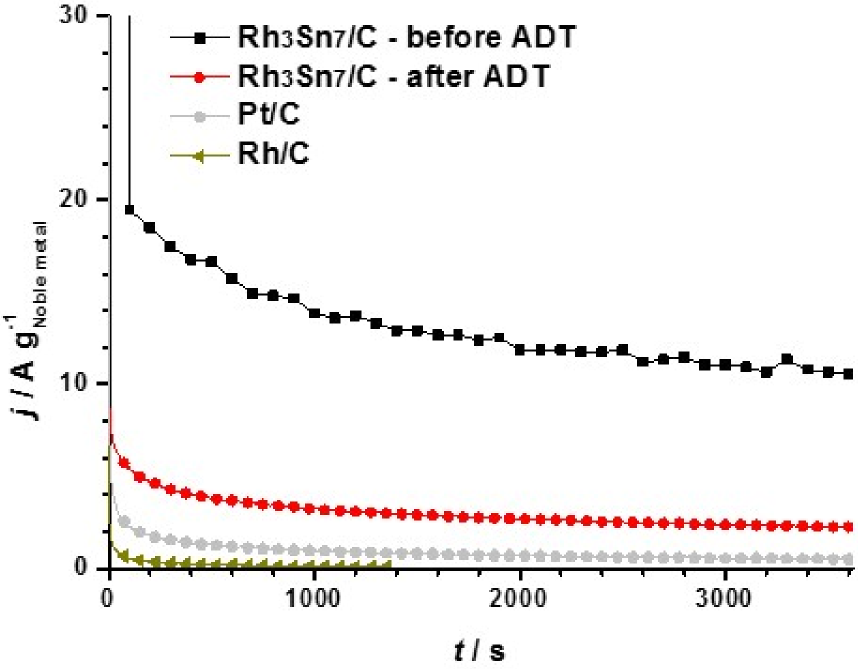

Figure S4. Chronoamperometry results of Rh_3Sn_7/C before and after accelerated stability test (1000 cycles, potential ranges from 0.6 V to 1.0 V, scan rate of 50 mV s^{-1}, oxygen-free electrolyte) and fresh monometallic catalysts at a constant potential of 0.3 V for 1 hour in 0.5 M ethanol solution.

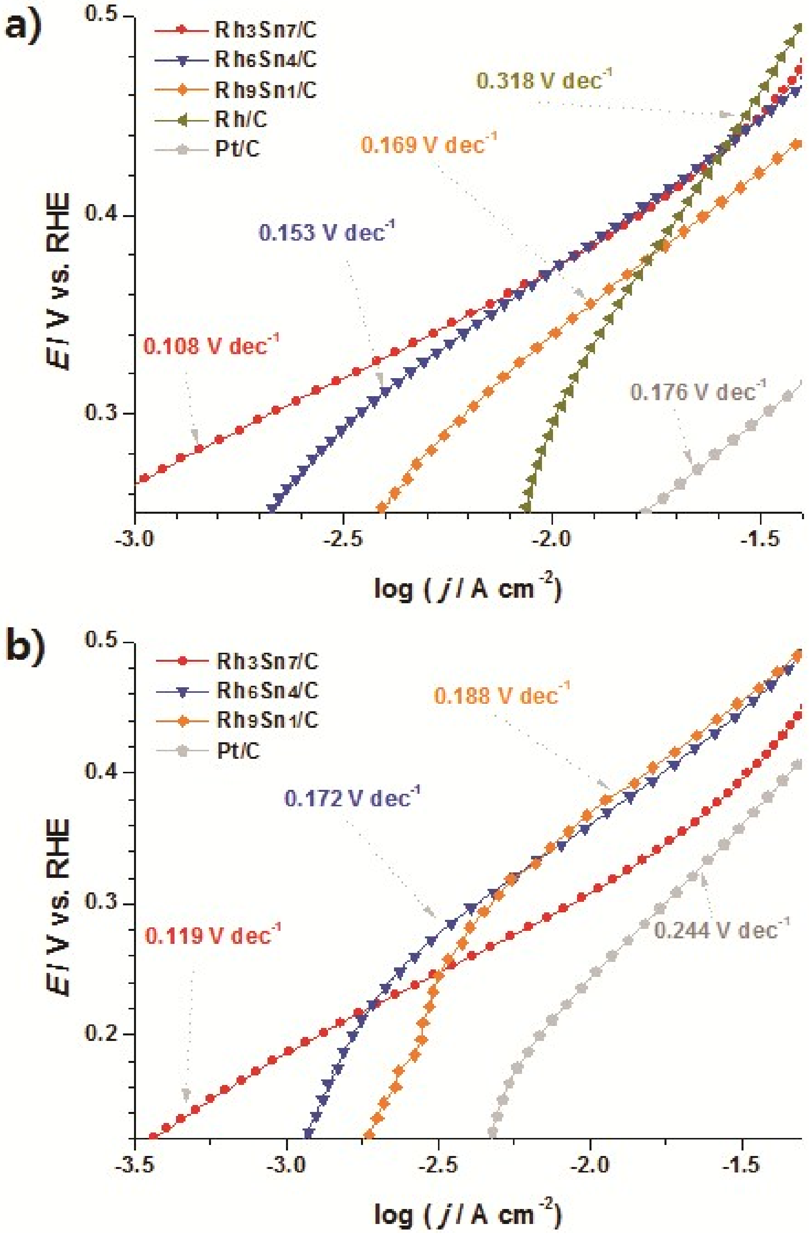

Figure S5. Tafel plots of Rh-Sn catalysts and commercial Pt catalyst in a) 0.5 M ethanol and b) 6.0 M ethanol electrolytes at a scan rate of 1 mV s^{-1}.

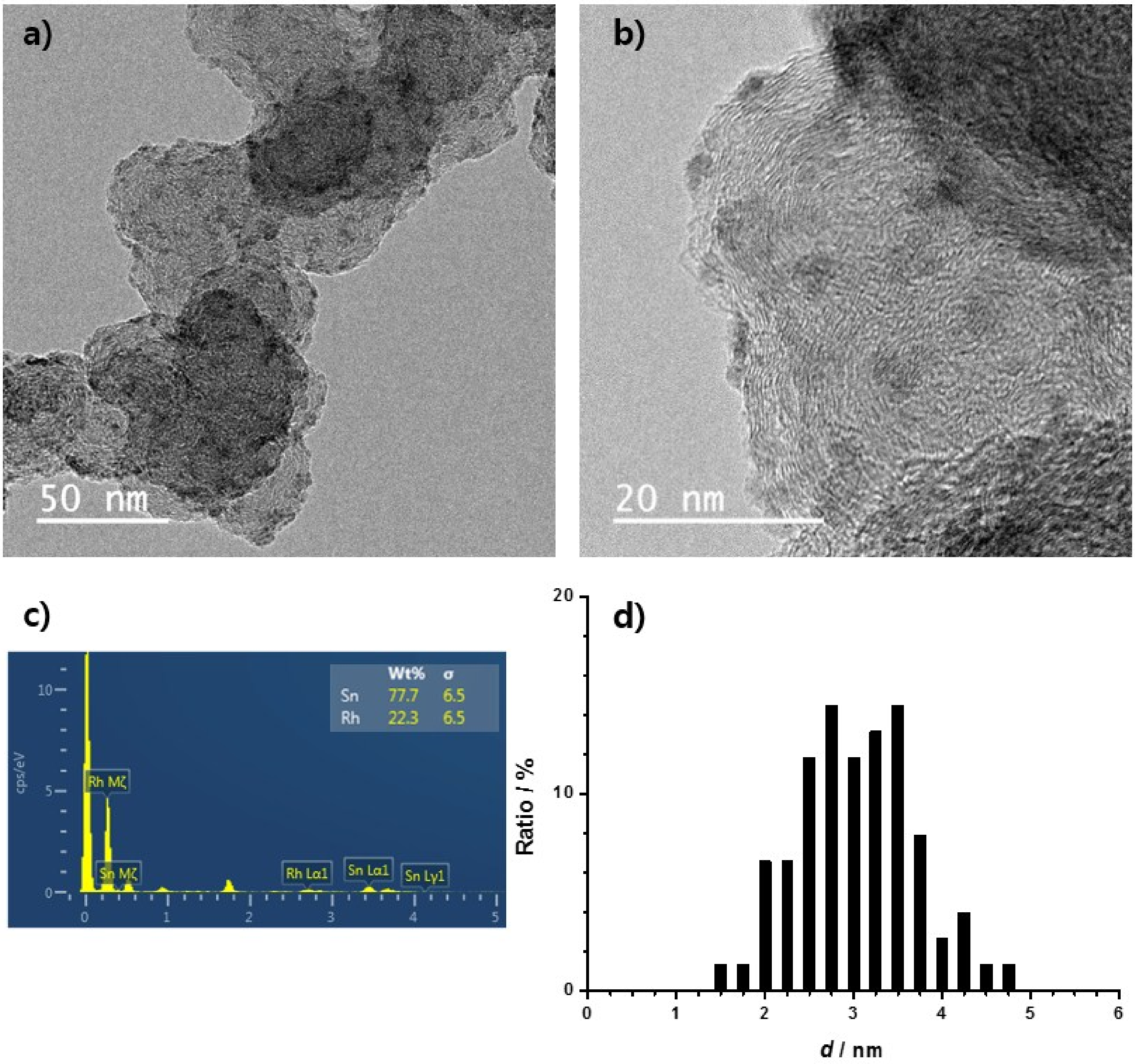

Figure S6. HR-TEM images with a) low- and b) high-magnification, c) atomic weight percent by EDS with area-scanning and d) particle size distribution of heterogeneous Rh_3Sn_7 nanoparticles supported on carbon.

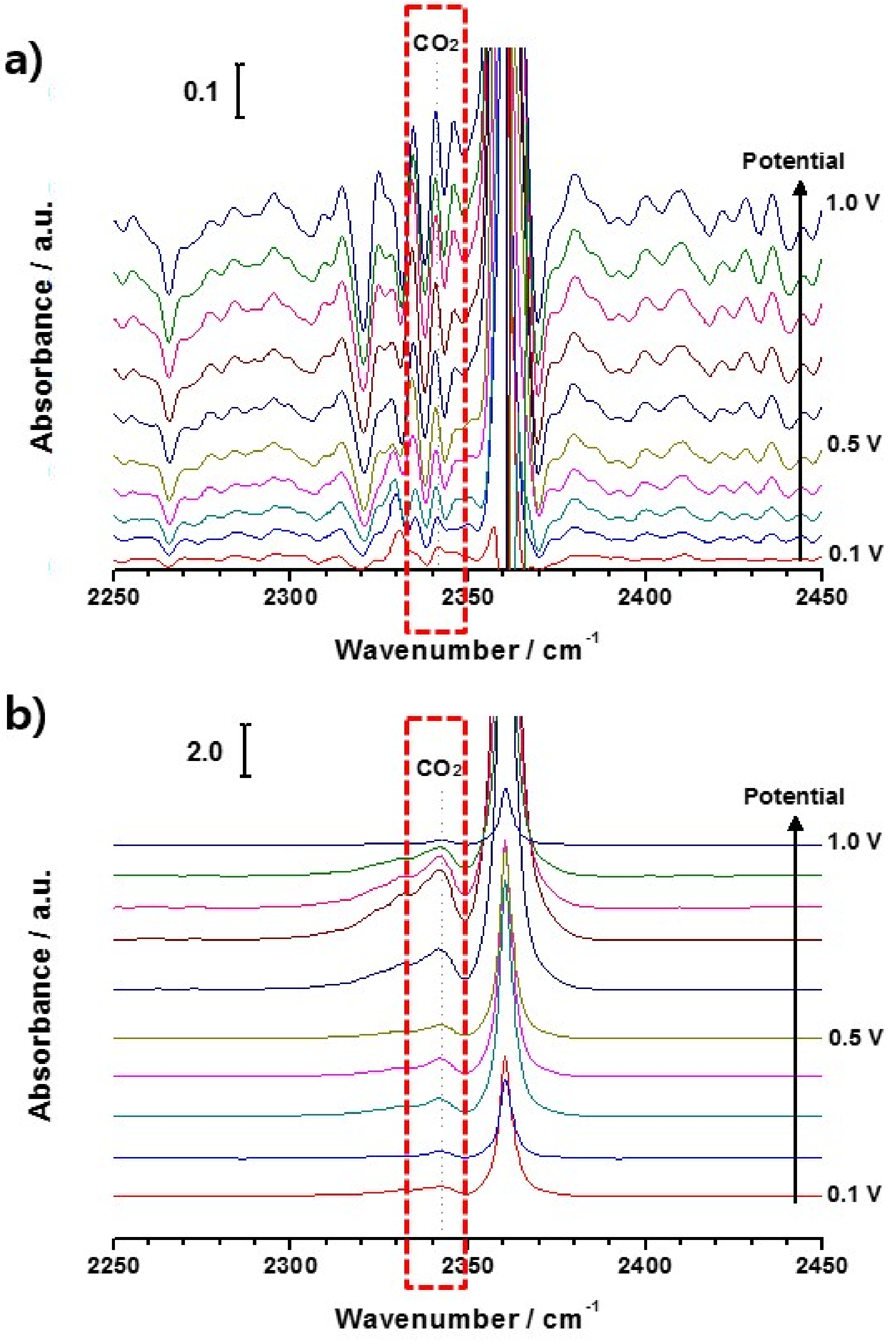

Figure S7. *in situ* ATR-FTIR spectra focused on CO_2 absorption band (2343 cm^{-1}) with potential profiles of a) Pt/C (J.M.) and b) Rh_3Sn_7/C. (Scale bar: a) 0.1 a.u., b) 2.0 a.u.)

Table S1. Summary of electrochemical and structural characteristics for conventional Pt/C and Rh_3Sn_7/C catalysts

Sample	Pt/C (J.M.)		Rh_3Sn_7/C	
Conditions	0.5 M fuel	6.0 M fuel	0.5 M fuel	6.0 M fuel
j_{mass} / A $g^{-1}_{noble\ metal}$	252.7	154.8	281.7	490.8
j_{area} / A m^{-2}	6.3	3.8	7.6	13.2
I_f/I_b	0.94	1.00	8.42	6.13
Tafel slope / V dec^{-1}	0.176	0.244	0.108	0.119
Average particle size / nm	2.8		3.0	
ECSA / m^2 g^{-1}	40.3		37.2	
Rh^0 at 630 eV / %	N/A		84.9	
Rh^0 at 1000 eV / %	N/A		95.2	
Sn^0 at 630 eV / %	N/A		0.1	
Sn^0 at 1000 eV / %	N/A		7.1	